Nanoscale Particle Motion in Attractive Polymer Nanocomposites

Erkan Senses,[1,2,*] Suresh Narayanan,[3] Yimin Mao,[1,2] and Antonio Faraone[1,†]
[1]NIST Center for Neutron Research, National Institute of Standards and Technology Gaithersburg, Maryland 20899-8562 USA
[2]Department of Materials Science and Engineering, University of Maryland College Park, Maryland 20742-2115 USA
[3]Advanced Photon Source, Argonne National Laboratory, Argonne, Illinois 60439, USA
(Received 17 July 2017; published 6 December 2017)

Using x-ray photon correlation spectroscopy, we examined the slow nanoscale motion of silica nanoparticles individually dispersed in an entangled poly (ethylene oxide) melt at particle volume fractions up to 42%. The nanoparticles, therefore, serve as both fillers for the resulting attractive polymer nanocomposites and probes for the network dynamics therein. The results show that the particle relaxation closely follows the mechanical reinforcement in the nanocomposites only at the intermediate concentrations below the critical value for the chain confinement. Quite unexpectedly, the relaxation time of the particles does not further slow down at higher volume fractions—when all chains are practically on the nanoparticle interface—and decouples from the elastic modulus of the nanocomposites that further increases orders of magnitude.

DOI: 10.1103/PhysRevLett.119.237801

Dispersing nanoparticles (NPs) into polymeric matrices results in unexpected and remarkable changes in macroscopic properties of the polymer-NP composites (PNCs) [1,2]. In PNCs, mechanical reinforcement is at the center of commercial interest [3] while interfacial polymer layer bound to NP surfaces [often called "bound layer" (BL)] is of great interest in the polymer physics community due to its distinct structural and dynamical properties relative to the free chains [4–9]. Linking the macroscopic reinforcement to the microscopic dynamics of the polymer chains and NPs in the PNCs remains a major challenge.

The viscoelastic properties of PNCs are primarily controlled by the polymer-NP interaction that also determines the NP dispersion state. On the one hand, it is the repulsive or neutral polymer-NP interaction that often leads to phase-separated or self-assembled superstructures [10,11] and their percolation within the soft matrix dominates the mechanical reinforcement [12–14]. On the other hand, favorable polymer-NP interaction facilitates polymer adsorption on NP surfaces and, in most cases, results in good dispersion of bare particles in polymers [15–18]. Elastic reinforcement in the absence of direct NP contact in these PNCs is beyond the predictions of the classical models [19]; the detailed mechanism is not well understood. For example, Long *et al.* [20,21] proposed a glassy layer surrounding NPs and explained the mechanical reinforcement by a percolation of overlapping frozen polymer fractions in a soft matrix at high NP volume fractions (ϕ_{NP}) or low temperature [22], although recent dynamic neutron scattering and dielectric experiments undeniably show that the BL can be internally highly mobile with no glassy nature [6,23,24]. More recently, using geometric arguments, Chen *et al.* [25] proposed a network model for NPs linked by flexible polymers at intermediate ϕ_{NP}, which transforms to glassy bridges at high ϕ_{NP} when interparticle distance becomes comparable to the Kuhn length (≈1 nm) of the chains [25,26].

Most of the proposed reinforcement mechanisms in attractive PNCs are primarily based on modification of the polymer mobility [27–29]; however, it is quite difficult to separate the dynamical processes of the highly interacting matrix and the interfacial chains. Meanwhile, the NPs essentially reflect the local viscoelastic properties of polymer in their nanoscale motion that is commonly measured by x-ray photon correlation spectroscopy (XPCS) [30–33]. To date, such experimental studies on the NP dynamics in PNCs have been limited to the dilute NP regime mainly due to the challenges in dispersing NPs in polymer melts at high ϕ_{NP} and the sensitivity of the particle dynamics on the morphology of resulting aggregates [34].

In this Letter, we take the first step to examine the slow, nanoscale motion of silica NPs uniformly dispersed in attractive poly (ethylene oxide) (PEO) melts well above the glass transition temperature $T > 1.7\,T_g$ at volume fractions, ϕ_{NP}, up to 42%. At such conditions, the NPs serve as both fillers and dynamic probes; their relaxation behavior allows us to observe the reinforcement in the PNCs from the "eyes" of the NPs.

The PEO ($M_w = 35$ kg/mol, $M_w/M_n = 1.08$), well above the entanglement molar mass, $M_e = 2$ kg/mol [35], was purchased from Polymer Source Inc. and dried further under vacuum at 363 K for 12 h. The silica NPs (≈24 nm in radius with size polydispersity ≈0.3) in methyl ethyl ketone were supplied by Nissan Chemicals America and used as received. To prepare the PNCs, PEO was first dissolved in acetonitrile at 30 mg/ml and NPs were added into polymer solution. The mixtures were sonicated for 20 min and then vigorously stirred for ≈2 h before casting. The samples were dried under a fume hood for ≈12 h and vacuum annealed at 363 K for 2 days and then at 393 K for

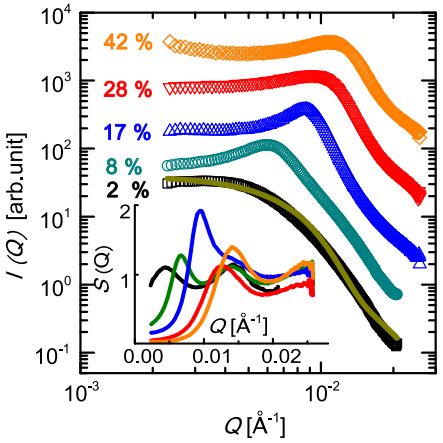

FIG. 1. SAXS profiles (shifted vertically for clarity) from the PNCs at 363 K. The line on $\phi_{NP} = 2\%$ is the fit result from spheres with radius of 24 nm and Gaussian size distribution of 0.3. The inset is the resulting structure factor peaks obtained by dividing the SAXS intensities by the fit results for the single particle form factor.

1 day for solvent removal. XPCS was performed on beam line 8-ID-I at the Advanced Photon Source at Argonne National Laboratory. The samples were molded at 363 K in 1 mm diameter and 0.8 mm thick spaces in aluminum plates and then annealed in a vacuum oven at 433 K for 1 h. The normalized intensity-intensity autocorrelation function g_2 (Q, t) was obtained over the wave vector range $0.003\ \text{Å}^{-1} < Q < 0.02\ \text{Å}^{-1}$. The measurements were repeated on five different locations on the samples; identical correlation functions were obtained. The beam attenuators for each sample were carefully selected to ensure the sample stability. Rheology experiments were performed on a strain-controlled ARES-G2 (TA instruments) rheometer equipped with 8 mm parallel plate fixtures.

Because of favorable interaction between PEO and Silica, NPs in PEO are well dispersed at all concentrations, up to $\phi_{NP} = 42\%$. Figure 1 displays their small-angle x-ray scattering (SAXS) profiles. For all PNCs, well-defined plateau are reached at low Q, suggesting the absence of structures larger than the single particle size. A slight intensity upturn at the lowest Q for $\phi_{NP} = 42\%$ is likely due to formation of large-scale particle network mediated by a bound polymer. At $\phi_{NP} = 2.5\%$, the intensity profile is described by the form factor of spheres $P(Q)$ (shown as the solid fit line) with an average radius of $R_{NP} = 24$ nm and size polydispersity of 0.3. At higher ϕ_{NP}, peaks appear at intermediate Q (Q^*) corresponding to average center-to-center NP distances, $L = 2\pi/Q^*$. The primary peak locations are clearly identifiable and shifted to higher Q in the structure factor $S(Q) = I(Q)/P(Q)$; plots shown in the inset of Fig. 1.

Table I displays the resulting face-to-face NP distances $h = L - 2R_{NP}$, calculated from SAXS peaks and the predictions from the random distribution of spheres

TABLE I. Nanocomposite characteristics, mass and volume fractions of NPs, face-to-face interparticle spacing and the confinement parameter.

NP% Mass (volume)	Face-to-face distance (h) [nm] SAXS	Random packing	$h/2R_g$
5 (2.5)	...	93.8	...
15 (7.8)	52.3	48.5	3.74
30 (17.1)	21.8	26.4	1.56
45 (28.3)	14.8	14.9	1.06
60 (41.9)	5.1	7.2	0.51

$2R_{NP}[(2/\pi\phi_{NP})^{1/3} - 1]$. A good agreement is found, further confirming the uniform and individual NP dispersion in the matrix. As the volume fraction increases, the geometric confinement parameter $h/2R_g$ ($R_g \approx 7$ nm as determined previously [36]) systematically decreases down to 0.5 (see Table I). The NP dispersion is stable against temperature as confirmed for all PNCs by their identical SAXS profiles (see Supplemental Material [37]). The distinct NP dynamics discussed herein are, therefore, not due to different aggregation states as demonstrated recently by Liu *et al.* [34] or local caging effects (see also Supplemental Material [37] for comparison of our aggregated and dispersed cases).

The slow NP motion was measured using XPCS over the length scale (20-200) nm and the time scale from 10 ms to 2000 s. The correlation function is related to the intermediate scattering function (ISF), $f(Q, t)$, as $g_2(Q, t) \sim 1 + A[f(Q, t)]^2$, with A and t being the Siegert factor of the instrument and the delay time, respectively. ISF is best fit to the stretched or compressed exponential functions $f(Q, t) = \exp[-(t/\tau)^{\beta}]$, with relaxation time τ and stretching or compressing exponent β. The simple exponential decay is indicative of diffusive motions while the compressed exponential decay is commonly associated with suppressed relaxation modes due to internal stresses and their sudden release as commonly observed in many jammed systems, gels, glass formers, and aggregated particles in polymer [12,30,38–42]. The results for all PNCs at 363 K and 423 K are displayed in Fig. 2. The correlation functions (shown for $Q \approx 0.01\ \text{Å}^{-1}$ in Fig. 2) shift to longer times with increasing ϕ_{NP}, suggesting slowing down of the NP dynamics. At $\phi_{NP} = 2.5\%$ and $\phi_{NP} = 8\%$, g_2 decays exponentially whereas g_2's are clearly compressed for $\phi_{NP} = 28\%$ and $\phi_{NP} = 42\%$ at both T. At $\phi_{NP} = 17\%$, the simple exponential decay at 433 K shifts to a more compressed form at 363 K. In order to test for any aging in the system, we measured XPCS on 20 different parts of the sample for 3 h (see Supplemental Material [37], Fig. S3); the overlapping profiles suggest no considerable dynamical aging at the length scales measured.

The Q dependence of the relaxation time is strongly concentration dependent. At $\phi_{NP} = 2.5\%$, the NPs are well separated $(h/2R_g \gg 1)$; thus, the isolated NPs exhibit

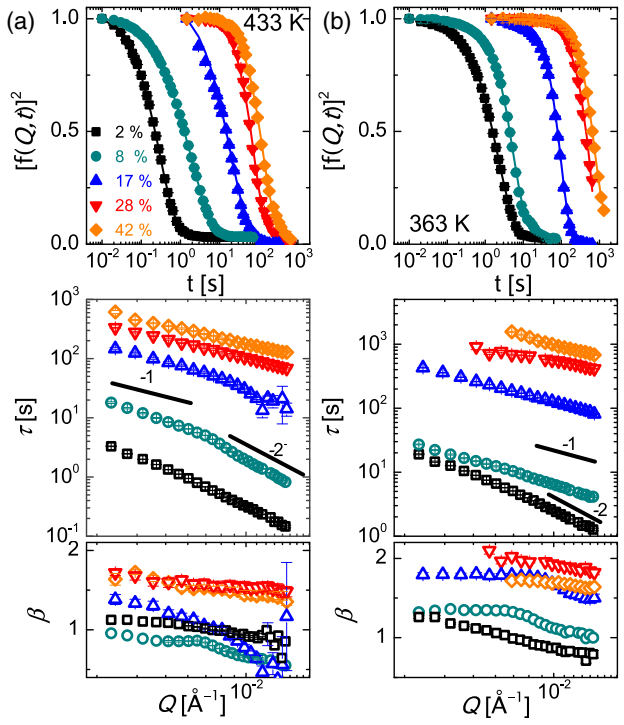

FIG. 2. XPCS intensity correlation functions at $Q = 0.01$ Å^{-1} (top figures) at (a) $T = 433$ K and (b) $T = 363$ K. The lines are the best fits to the stretched exponential forms that result in relaxation times (τ) and stretching exponent (β) displayed. The lines in the $\tau(Q)$ plots show the trends for simple diffusive, $\tau \propto Q^{-2}$, and ballistic $\tau \propto Q^{-1}$ motions. Error bars represent one standard deviation.

simple diffusion with $\beta \approx 1$ and $\tau \propto Q^{-2}$ scaling. This is consistent with an earlier report by Guo *et al.* [30] where tracer NPs exhibit simple diffusion in an unentangling polystyrene melt at $T > 1.2\,T_g$ while the NPs are hyperdiffusive at lower T due to dynamic heterogeneities associated with the glass transition of the matrix. Our measurements were performed at $T > 1.7\,T_g$ where PEO is a viscous liquid in the time scale of XPCS ($t_{\mathrm{XPCS}} >$ 10 ms $> t_d$, where t_d is the terminal relaxation time [43]); the NPs are expected to exhibit simple diffusion. The local viscosity estimated from the Stokes-Einstein relation $\eta_{\mathrm{XPCS}} = k_B T/(6\pi D_{\mathrm{NP}} R_{\mathrm{NP}})$ where $D_{\mathrm{NP}} = 1/(\tau Q^2)$ is ≈260 Pa s, close to the bulk viscosity of PEO at $T =$ 363 K [36].

On the other extreme, at $\phi_{\mathrm{NP}} \approx 42\%$ and $h/2R_g < 1$, all polymer chains are practically in direct contact with the NPs; thus, the response is solely from NPs with overlapping bound chains. Note that the NPs adsorb polymer in the solution phase where NP-NP distance is orders of magnitude larger than the interparticle distance in the solvent-free PNCs; the NPs are not directly bridged by the BL, rather BLs interact with their loop and tails. In this case, the relaxation becomes extremely slow and hyperdiffusive with $\tau \propto Q^{-1}$ and $\beta \approx 1.5 - 2$ at all temperatures (see Supplemental Material [37] for other temperatures). Note that the PNC with $\phi_{\mathrm{NP}} \approx 28\%$ is at the limit of $h/2R_g \approx 1$ and presents a similar hyperdiffusive behavior but with faster relaxation times compared to $\phi_{\mathrm{NP}} \approx 42\%$.

The intermediate concentrations present the features of both dilute and concentrated PNCs depending on the temperature and Q. This is clearly seen in PNC with $\phi_{\mathrm{NP}} = 8\%$. At $T = 363$ K, β is compressed around 1.5 with $\tau \propto Q^{-1}$ while it becomes close to unity at 433 K. More interestingly, there is a crossover of τ behavior between diffusive ($\tau \propto Q^{-2}$) and hyperdiffusive ($\tau \propto Q^{-1}$) at a length scale corresponding to $2\pi/Q^* \approx 100$ nm, matching the average center-to-center distance (Q^*) of the NPs (Table I). Similar behavior is also observed for $\phi_{\mathrm{NP}} \approx 17\%$: $\beta(T = 363\ \mathrm{K}) \approx 1.5$–2 and $\beta(T = 433\ \mathrm{K}) \approx 1$ with crossover observed at a length scale $2\pi/Q^* \approx 70$ nm. As the NPs serve as the junction points in a polymer mediated NP network, the length scale associated with the network dynamics is determined by distance between the particles and separate simple diffusive and slower hyperdiffusive regions.

We now compare the observed NP dynamics with the rheological properties of the PNCs. Figure 3(b) shows the elastic (G') and viscous (G'') moduli at 363 K. The neat liquidlike PEO gradually transforms to a gel-like (less frequency dependent) PNC with increasing ϕ_{NP}. The moduli vary monotonically within 7 orders of magnitude relative to the neat polymer in the terminal flow regime and the G' determined at $\omega = 0.1$ rad/s is displayed in Fig. 3(c). Note that for intermediate ϕ_{NP}, the crossover between the G' and G'' is observed within the time scale of the rheological experiments (≈20 ms to 100 s) that is on the same order of the XPCS time scale.

The fact that there is no direct NP contact in PNCs and that the neat PEO is in its viscous flow regime (reptation time, $t_d \approx 1\ \mathrm{ms} \ll 1/\omega_{\mathrm{min}}$) with negligible elasticity demand an additional, ϕ_{NP} dependent elastic network in PNCs. Such an elastic network in attractive PNCs is due to pinned chains on attractive NP surfaces. Long *et al.* [20,21] proposed that the bound polymer layer is glassy and the reinforcement is explained by the percolation of these glassy fractions in a soft matrix [22]. Recent dynamic neutron scattering and dielectric experiments showed that the bound chains are in fact internally highly mobile with no glassy nature [6,23,24] while their center-of-mass diffusion and some Rouse modes are suppressed due to adsorption [23,24]. The loops of the bound chains entangle with the surrounding—otherwise free—chains forming an interphase that propagate the dynamic slowing down of the interfacial chains further into the matrix.

Chen *et al.* [25] recently developed a parameter independent model to explain the reinforcement in attractive P2VP-silica PNCs with different NP sizes. The reinforcement at intermediate ϕ_{NP} was based on formation of a network of NPs that are bridged by flexible bound chains.

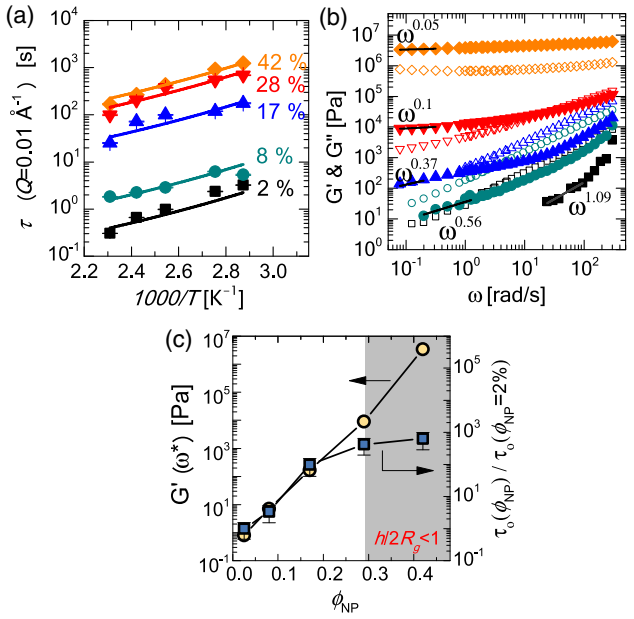

FIG. 3. (a) Temperature dependence of the NP relaxation times (τ) in PNCs. The lines are the best fits to VFT equation with the known PEO parameters (see the text). (b) Linear elastic (G', filled symbols) and viscous (G'', open symbols) moduli as a function of deformation frequency at 363 K showing liquid-to-elastic transition in the PNCs with increasing ϕ_{NP}. (c) Relaxation times obtained from the VFT fits shown in (a) and the elastic moduli of PNCs obtained determined at $\omega = 0.1$ rad/s. The shaded area indicates the region where face-to-face NP distance separation (h) is smaller than the chain size ($2R_g$). Error bars represent one standard deviation.

In their model, 25 nm sized NPs form a rubbery and flexible bridge at $\phi_{NP} \approx (5\text{–}45)\%$ and the bridges are glassy at $\phi_{NP} > 45\%$ as in Refs. [20,21]. Using temperature dependent rheological shift factors, Baeza *et al.* [26] showed a networklike response on the same system. The underlying hypothesis in both is that the interparticle distance is not uniform and the networklike response is seen when the mean distance between nearest neighbors (h) is between one Kuhn length (≈1 nm) and the chain size. Glasslike dynamics with Arrhenius type temperature dependence [26] was found at higher loadings.

We then looked at the temperature dependence of the relaxation times. The NPs at all ϕ_{NP} show similar temperature dependence [shown in Fig. 3(a) for $Q = 0.01$ Å^{-1}] that are well described by the Vogel-Fulcher-Tamman (VFT) equation $\tau(T) = \tau_o \exp[B/(T - T_\infty)]$ with known $B = 1090$ and $T_o = 155$ K for PEO [44]. We have not seen any distinct change in the temperature dependence with NPs concentrations. Also, the trends obtained from the fitting were similar at the high- and low-Q regimes (see Supplemental Materials [37]). The high T limit of the relaxation time τ_o increases orders of magnitude with ϕ_{NP} up to 28% (where $h/2R_g > 1$) in close agreement with the observed mechanical reinforcement. However, adding more NPs does not further slow down the dynamics even if the interparticle separation becomes smaller than the chain size; the NPs at $\phi_{NP} = 42\%$ are almost as mobile as at $\phi_{NP} = 28\%$ (Fig. 3(c) and see Supplemental Material [37]). The observed trend in NPs is in contrast with the observed 3 orders of magnitude increase of elastic modulus in the PNCs; the NP and bulk mechanical relaxation decouple near and above the critical chain confinement. We attribute this to the presence of bound chains on NPs, which are not frozen, and allows motion of the NPs through segmental relaxation of the loops and tails of the BL. In the absence of the "free" chains at high ϕ_{NP}, the NPs experience the same viscoelastic environment and their relaxation reaches a plateau.

The sharp transition from diffusive to hyperdiffusive relaxation at intermediate concentrations [Fig. 2(a)] suggests that there is a certain length scale associated with the NP network above which the NPs feel the network. Our results suggest that this length scale can be as high as $7\,R_g$ for $\phi_{NP} = 8\%$ [crossover in relaxation time in Fig. 2(a)]. The elastic network, at least in this work, is not due to bridging of NPs by a single bound polymer, rather because of interchain effects between the surface bound and the free polymer that direct the NP slowing down. This is consistent with the observation by Winey and co-workers suggesting that the center-of-mass diffusion of the long chains indeed starts to decrease in attractive PNCs at $h/2R_g \approx 8$ and the diffusion of large NPs are slowed down accordingly [45–47]. These results provide strong evidence that the chain-chain entanglements—which have not been the focus of earlier studies—could play a significant role in determining component dynamics in PNC melts. We conjecture that our findings in the melt state may also apply on the attractive PNCs in a swollen state at time scales shorter than the life time of BL. The response at longer times would be similar to the behavior of concentrated NPs in nonattractive and entangled polymer solutions [48].

In conclusion, using XPCS, we studied the nanoscale motion of attractive bare-silica nanoparticles in entangled PEO melts at high concentrations relevant to polymer nanocomposites. Both diffusive and hyperdiffusive behavior was observed depending on the NPs concentration, temperature, and probed length scale. The relaxation of NPs slows down, in parallel with the enhanced composite moduli, only in the region where the face-to-face distance is larger than the chain size and where the chain-chain topological interactions are important. Above this concentration, the NP motion is not further slowed down despite 3 orders of magnitude increase in the elastic moduli of the PNC. The results suggest that interfacial chains are highly mobile in PNCs and allow motion of NPs independent of the viscoelastic reinforcement of the PNCs in the strong confinement limit. These new experimental results call for rethinking the existing reinforcement mechanism in PNCs and NP motion in molten polymers.

This work used resources of the Advanced Photon Source, a U.S. Department of Energy (DOE) Office of Science User Facility operated for the DOE Office of Science by Argonne National Laboratory under Contract No. DE-AC02-06CH11357. The identification of any commercial product or trade name does not imply endorsement or recommendation by the National Institute of Standards and Technology. We thank Dr. Paul Butler and Dr. Hongyu Guo for valuable discussions and the Security Technologies Group of NIST for the use of rheometer.

*erkan.senses@nist.gov
†antonio.faraone@nist.gov

[1] R. Krishnamoorti and R. A. Vaia, *Polymer Nanocomposites: Synthesis, Characterization, and Modeling* (American Chemical SocietyWashington, DC, 2002), Vol. 804.
[2] M. Moniruzzaman and K. I. Winey, Macromolecules **39**, 5194 (2006).
[3] S. K. Kumar, B. C. Benicewicz, R. A. Vaia, and K. I. Winey, Macromolecules **50**, 714 (2017).
[4] S. E. Harton, S. K. Kumar, H. Yang, T. Koga, K. Hicks, H. Lee, J. Mijovic, M. Liu, R. S. Vallery, and D. W. Gidley, Macromolecules **43**, 3415 (2010).
[5] N. Jiang, M. K. Endoh, T. Koga, T. Masui, H. Kishimoto, M. Nagao, S. K. Satija, and T. Taniguchi, ACS Macro Lett. **4**, 838 (2015).
[6] A. P. Holt, P. J. Griffin, V. Bocharova, A. L. Agapov, A. E. Imel, M. D. Dadmun, J. R. Sangoro, and A. P. Sokolov, Macromolecules **47**, 1837 (2014).
[7] F. W. Starr, J. F. Douglas, D. Meng, and S. K. Kumar, ACS Nano **10**, 10960 (2016).
[8] S. Sen, Y. Xie, S. K. Kumar, H. Yang, A. Bansal, D. L. Ho, L. Hall, J. B. Hooper, and K. S. Schweizer, Phys. Rev. Lett. **98**, 128302 (2007).
[9] F. W. Starr, T. B. Schrøder, and S. C. Glotzer, Macromolecules **35**, 4481 (2002).
[10] P. Akcora *et al.*, Nat. Mater. **8**, 354 (2009).
[11] L. M. Hall, A. Jayaraman, and K. S. Schweizer, Curr. Opin. Solid State Mater. Sci. **14**, 38 (2010).
[12] P. Akcora *et al.*, Macromolecules **43**, 1003 (2010).
[13] D. Zhao, S. Ge, E. Senses, P. Akcora, J. Jestin, and S. K. Kumar, Macromolecules **48**, 5433 (2015).
[14] Z. Zhu, T. Thompson, S.-Q. Wang, E. D. von Meerwall, and A. Halasa, Macromolecules **38**, 8816 (2005).
[15] E. Senses and P. Akcora, Macromolecules **46**, 1868 (2013).
[16] E. Senses, A. Isherwood, and P. Akcora, ACS Appl. Mater. Interfaces **7**, 14682 (2015).
[17] G. P. Baeza *et al.*, Nat. Commun. **7** (2016).
[18] S. Cheng *et al.*, Phys. Rev. Lett. **116**, 038302 (2016).
[19] G. K. Batchelor, J. Fluid Mech. **83**, 97 (1977).
[20] J. Berriot, H. Montes, F. Lequeux, D. Long, and P. Sotta, Macromolecules **35**, 9756 (2002).
[21] D. Long and F. Lequeux, Eur. Phys. J. E **4**, 371 (2001).
[22] S. Merabia, P. Sotta, and D. R. Long, Macromolecules **41**, 8252 (2008).
[23] M. Krutyeva *et al.*, Phys. Rev. Lett. **110**, 108303 (2013).
[24] T. Glomann, G. J. Schneider, J. Allgaier, A. Radulescu, W. Lohstroh, B. Farago, and D. Richter, Phys. Rev. Lett. **110**, 178001 (2013).
[25] Q. Chen, S. Gong, J. Moll, D. Zhao, S. K. Kumar, and R. H. Colby, ACS Macro Lett. **4**, 398 (2015).
[26] G. P. Baeza *et al.*, Nat. Commun. **7**, 11368 (2016).
[27] K. Nusser, S. Neueder, G. J. Schneider, M. Meyer, W. Pyckhout-Hintzen, L. Willner, A. Radulescu, and D. Richter, Macromolecules **43**, 9837 (2010).
[28] K. Nusser, G. J. Schneider, and D. Richter, Soft Matter **7**, 7988 (2011).
[29] Y. Golitsyn, G. J. Schneider, and K. Saalwächter, J. Chem. Phys. **146**, 203303 (2017).
[30] H. Guo, G. Bourret, M. K. Corbierre, S. Rucareanu, R. B. Lennox, K. Laaziri, L. Piche, M. Sutton, J. L. Harden, and R. L. Leheny, Phys. Rev. Lett. **102**, 075702 (2009).
[31] T. Koga, N. Jiang, P. Gin, M. K. Endoh, S. Narayanan, L. B. Lurio, and S. Sinha, Phys. Rev. Lett. **107**, 225901 (2011).
[32] R. L. Leheny, Curr. Opin. Colloid Interface Sci. **17**, 3 (2012).
[33] J. Liu, M. L. Gardel, K. Kroy, E. Frey, B. D. Hoffman, J. C. Crocker, A. R. Bausch, and D. A. Weitz, Phys. Rev. Lett. **96**, 118104 (2006).
[34] S. Liu, E. Senses, Y. Jiao, S. Narayanan, and P. Akcora, ACS Macro Lett. **5**, 569 (2016).
[35] L. Fetters, D. Lohse, and R. Colby, in *Physical Properties of Polymers Handbook*, edited by J. E. Mark (Springer, New York, 2007), pp. 447.
[36] E. Senses, S. M. Ansar, C. L. Kitchens, Y. Mao, S. Narayanan, B. Natarajan, and A. Faraone, Phys. Rev. Lett. **118**, 147801 (2017).
[37] See Supplemental Material at http://link.aps.org/supplemental/10.1103/PhysRevLett.119.237801 for particle dynamics in clustered states, aging study and Q-dependence of relaxation time.
[38] L. Cipelletti, L. Ramos, S. Manley, E. Pitard, D. A. Weitz, E. E. Pashkovski, and M. Johansson, Faraday Discuss. **123**, 237 (2003).
[39] A. Madsen, R. L. Leheny, H. Guo, M. Sprung, and O. Czakkel, New J. Phys. **12**, 055001 (2010).
[40] H. Guo, J. N. Wilking, D. Liang, T. G. Mason, J. L. Harden, and R. L. Leheny, Phys. Rev. E **75**, 041401 (2007).
[41] H. Guo, S. Ramakrishnan, J. L. Harden, and R. L. Leheny, Phys. Rev. E **81**, 050401 (2010).
[42] B. Ruta, O. Czakkel, Y. Chushkin, F. Pignon, R. Nervo, F. Zontone, and M. Rinaudo, Soft Matter **10**, 4547 (2014).
[43] E. Senses, A. Faraone, and P. Akcora, Sci. Rep. **6**, 29326 (2016).
[44] K. Niedzwiedz, A. Wischnewski, W. Pyckhout-Hintzen, J. Allgaier, D. Richter, and A. Faraone, Macromolecules **41**, 4866 (2008).
[45] P. J. Griffin, V. Bocharova, L. R. Middleton, R. J. Composto, N. Clarke, K. S. Schweizer, and K. I. Winey, ACS Macro Lett. **5**, 1141 (2016).
[46] W.-S. Tung, P. J. Griffin, J. S. Meth, N. Clarke, R. J. Composto, and K. I. Winey, ACS Macro Lett. **5**, 735 (2016).
[47] C.-C. Lin, S. Gam, J. S. Meth, N. Clarke, K. I. Winey, and R. J. Composto, Macromolecules **46**, 4502 (2013).
[48] R. Poling-Skutvik, K. I. S. Mongcopa, A. Faraone, S. Narayanan, J. C. Conrad, and R. Krishnamoorti, Macromolecules **49**, 6568 (2016).